Photocatalytic Hydrogen Production under Visible Light over Magnesium Ferrite

V. Guzmán-Velderrain[1], M. Meléndez Zaragoza[1], E. Medina-Henandez[2], P. Gutiérrez Rivera[3], L. García Campos[1], Y. Ortega-López[1], J. Salinas Gutiérrez[1], A. López Ortiz[1], V. Collins-Martínez[1*]

[1]Centro de Investigación en Materiales Avanzados S. C., Laboratorio Nacional de Nanotecnología, Depto. de Materiales Nanoestructurados, Miguel de Cervantes 120, C. P. 31109, Chihuahua, Chih. México
[2]Universidad Autónoma de Chihuahua, Facultad de Ciencias Químicas, Campus Universitario # 2 C.P. 31125, Chihuahua, Chih, México
[3]Universidad Tecnología Junta de los Ríos, Carretera Aldama, Km 3, C. P. 31313, Chihuahua, Chih. México
. Tel: +52 (614)439 11 29 *e mail: virginia.collins@cimav.edu.mx

ABSTRACT

Magnesium ferrite ($MgFe_2O_4$) was synthesized by the hydrothermal technique and was found to be an active photocatalyst for hydrogen production from water under visible light. The structural, morphological, and optical properties of the material were characterized by powder XRD, SEM, TEM, and UV-Vis diffuse reflectance spectroscopy. Iron and magnesium aqueous nitrate solutions were used as precursors under hydrothermal conditions of 200 °C for 3.5 h. $MgFe_2O_4$ photocatalytic activity towards the H_2 production was determined by gas chromatography, using a batch-type quartz photoreactor and irradiated using a 250 W mercury lamp. XRD results from the synthesized sample found the $MgFe_2O_4$ crystalline structure. The optical properties revealed semiconducting properties with a band gap energy (E_g) of 2.07 eV (599nm) showing an efficient visible light absorption. SEM images found particles with a morphology in the form of agglomerates composed of hemispherical particles, while TEM images revealed particles with an average of 9.3 nm in size. Furthermore, the solid exhibited a high photoactivity toward the reduction of water, which is attributed to the efficient separation and transportation of the photogenerated charge carriers. This ferrite material exhibited a production of 650 µmol $H_2/g_{catalyst}$ over an irradiation period of 8 h, thus exceeding the H_2 generation obtained by TiO_2, which was of 15 µmol $H_2/g_{catalyst}$. This increase in H_2 production is attributed to the fact that $MgFe_2O_4$ exhibits a band gap, which is activated under the visible light range.

Keywords: Hydrogen production, $MgFe_2O_4$, Water splitting

1. Introduction

In the last decade it has been an increased research interest related to renewable energy, because of environmental constraints and the low efficiency offered by traditional fossil energies. It is thought that the development of a new sources of renewable energy will bring a number of advantages [1]. A promising alternative is the use of hydrogen, because it has so many desirable features such as clean emissions when used as fuel, abundance, accessibility, high efficiency and overall versatility of use [2]. However, the first step in the production of a safe and clean energy, is finding a method for producing hydrogen cheaply and efficiently [1]. Currently, hydrogen is proposed as an energy vector that can be applied to renewable energy source (RES) such as solar, wind, biological, ocean and geothermal. Of these alternative RES it is important to take in to account factors like accessibility, affordability and being environmentally friendly. Based on this the use of water can be considered as an ideal source of hydrogen [3, 4, 5, 6, 7].

In the literature there are reports of hydrogen production from water photo reduction in the presence of semiconductors (SC) as photocatalysts. That is why the exploration of new semiconductors with high photocatalytic activity under visible light irradiation, projected various advantages such as low cost, favorable positioning of the band energy levels and chemical stability in aqueous media [8].

Ferrites with the general formula MFe_2O_4, where (M) represents a metal cation have various applications because of their chemical and thermal stability. Their applications mainly has excelled in electronic devices and circuits, besides their increasing use as absorbers of toxic and hazardous substances to health. Ferrites have shown to be effective photocatalysts under visible light to generate electron-hole pairs on the photocatalytic material surface. However, there is still a great challenge in understanding the mechanisms of water reduction [9].

Magnesium Ferrite ($MgFe_2O_4$) has a band gap energy of 2.18 eV [9], indicating that it can be activated under the visible light range. Literature reports several synthesis methods for preparing the magnesium ferrite spinel, such as ceramic [10-12], hydrothermal [13], sol-gel [14], citrate gel [15], combustion [16 - 17], mechanical alloying [18], coprecipitation [19], etc. However, the coprecipitation method has some advantages such as: simple, fast, easy control of particle size and composition and various possibilities for controlling the state of the total surface of the particles and their homogeneity. Generally, after performing coprecipitation, the material is exposed to a heat treatment to crystallize, but runs the risk of particle growth and then exceed the nanometer scale. Therefore, in the present work the precipitation is to be combined with hydrothermal treatment to obtain a material with all the above mentioned advantages of the coprecipitation method, while keeping the particles in a nanometric size through the use of the hydrothermal treatment.

The objective of this work is to synthesize magnesium ferrite by the coprecipitation combined with hydrothermal treatment, characterize their structural, morphological, textural and optical properties, and to evaluate its photocatalytic activity towards the hydrogen production under visible light.

2. Experimental

2.1. Synthesis of nanoparticles

Precursor solutions were synthesized by the coprecipitation/hydrothermal method, using precursors: Magnesium II nitrate ($Mg(NO_3)_2*4H_2O$) Sigma Aldrich brand with a 98% purity and Iron III nitrate ($Fe(NO_3)_3*9H_2O$) Sigma Aldrich brand with a purity of 98%. The material was prepared in order to obtain 1 g of $MgFe_2O_4$, for that 4.39 g of $Fe(NO_3)_3*9H_2O$ was added in 5 ml of water and 1.39 g of $Mg(NO_3)_2$ in 3 ml of water. These solutions were mixed and placed in a burette and allowed to drip into 20 ml of ammonium hydroxide (NH_4OH) as a precipitating agent and pH regulated to a value of approximately 10. Subsequently, the mixture was exposed to a hydrothermal treatment in an autoclave using a Teflon vial at 200 °C for 3 h.

2.2. Material Characterization

$MgFe_2O_4$ powders were characterized by different techniques in order to study its physical and chemical characteristics. In order to determine the crystal structure of the material, this was analyzed by XRD using a Bruker D8 Advance model X-ray diffractometer with a 1.54060Å wavelength and employing 15 to 85 ° in 2θ with a step-size of 0.05 and 120s by step. The crystal size was estimated using the Scherrer's equation. The light absorption spectra of the material was acquired by UV/Vis diffuse reflectance spectra using a Perkin Elmer (Lambda-10) spectrometer equipped with an integrating sphere. The photocatalyst morphology was examined by transmission electron microscopy (TEM), in addition the particle size thereof was measured by a particle counting on a JEM-2200FS transmission electron microscope of ultra-high resolution that combines an emission gun of 200kV with an omega filter. The surface area of the powders was evaluated by the nitrogen physisorption technique (BET) to a degassing temperature of 180 °C, using a Quantachrome Autosorb-1 BET aparatus.

2.3. Photocatalytic Evaluation

200 mg of $MgFe_2O_4$ nanoparticles were suspended in water and methanol, the latter was used as a sacrificial agent; the suspension was placed inside a quartz batch type photoreactor (Figure 1) with a length of 19 cm and a diameter of 5 cm, which was sealed and located 7 cm away from a 250W mercury lamp. Hydrogen production was monitored using a gas chromatograph Perkin Elmer Clarus 500. Photocatalytic activity was evaluated over a period of time of 8 hours with sampling intervals of every hour.

Since titanium dioxide (TiO_2) is a reference photocatalyst, TiO_2 was synthesized by the sol-gel method assisted with hydrothermal treatment (TiO_2-F), both physical and chemical properties as well as the photocatalytic activity towards the hydrogen production were compared via the dissociation of the water molecule.

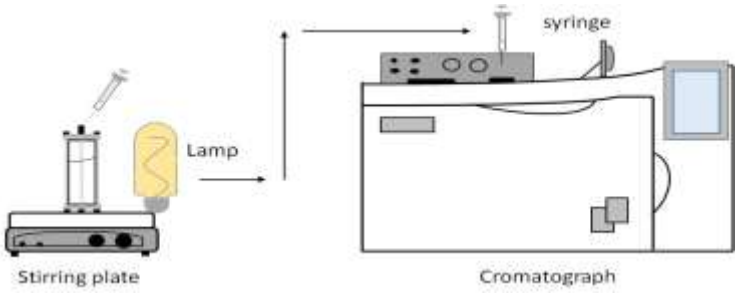

Fig 1. Diagram for the photocatalytic evaluation process

3. Results and discussion

3.1. Difracción de Rayos X

In Figure 2 the X-ray diffractograms of the $MgFe_2O_4$ and TiO_2-F photocatalysts are shown. From them the diffraction angles of the crystalline structures present in the materials can be observed. For the MgFe2O4 sample a mixture of phases was observed; α-Fe_2O_3 and the spinel $MgFe_2O_4$. Observing the diffraction angles of 33.4 °, 42.2 °, 57.5 °, 63 ° which correspond to the reflections (311), (400), (511) and (440) of cubic $MgFe_2O_4$. While angles 24.3 °, 33.1 °, 40.8 °, 49.3 °, 54.1 ° correspond to reflections (012), (104), (113), (024) and (116) that identify the phase α-hematite Fe_2O_3 [20]. The result of the phase mixture can be explained since the phase diagram Fe_2O_3-MgO-O_2 (P, atm) indicates that at stoichiometric ratios and low temperatures a single-phase mixture is reached as presently obtained.

For the case of TiO_2-F peaks located at 25.4, 37.8, 48.0, 54.5 ° of 2 Θ the corresponding to planes (101), (004), (200), (105 and 211) of the anatase phase are observed [22].

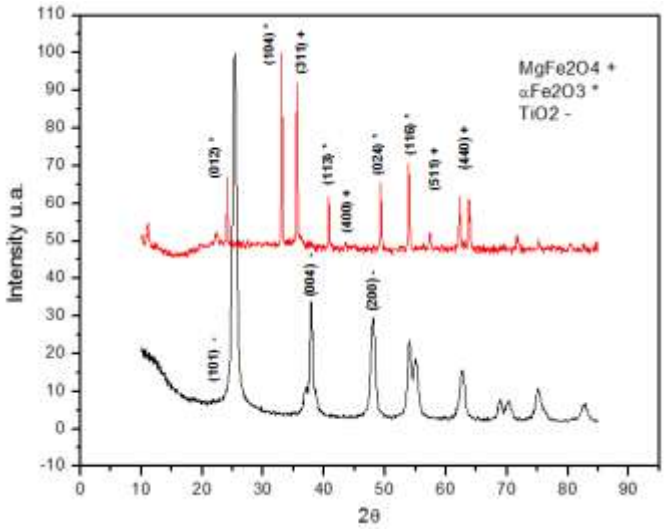

Fig 2. $MgFe_2O_4$ and TiO_2-F sample diffraction patterns.

Comparing the width of the peaks of the TiO_2-F and $MgFe_2O_4$ and sample it can be observed that narrower signals for the ferrite, suggesting a greater crystal size for this sample. To determine the crystal size of the samples X-ray patterns data (characteristic peak of each material) and the Scherrer's equation was employed, thus TiO_2-F presented a crystal size of 10.5 nm, while $MgFe_2O_4$ showed a size of 44 nm, which proves the earlier assumption about the width of the diffraction patterns peaks. This difference in crystal size can be attributed to the different synthesis methods used in each material (different mechanisms of nucleation and growth), coprecipitation for ferrite and sol-gel for the titanium oxide.

3.2. UV-Vis Spectroscopy

UV-Vis diffuse reflectance spectra for $MgFe_2O_4$ and doped TiO_2-F converted to Kubelka Munk units are presented in Figure 3. To determine the sample band gap it was considered a linear trend from inflection region of the spectrum, which represents the energy absorption over the edge. Extrapolating the slope of the linear region to intercept the photon energy axis (x-axis), this point provides the value of optical band gap of the material.

In this Figure it can be seen that the value of energy band gap (Eg) for the TiO_2-F sample is 3.12eV, which is very close to the reported value for the TiO_2 anatase phase of 3.2 eV [22]. On the other hand sample $MgFe_2O_4$ presents an Eg value of 2.07eV. This value is within the values reported for magnesium ferrite spinel which are between 2.0 and 2.18 eV, and these vary depending on the particle size; the smaller the value of the band gap this increases [9].

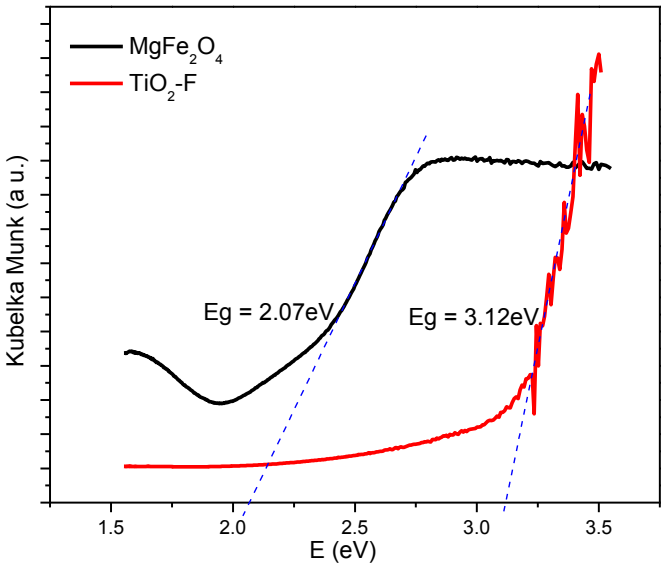

Fig 3. Band gap determination by UV-Vis spectroscopy.

3.3. Transmission electron Microscopy (TEM)

Transmission electron microscopy images for samples $MgFe_2O_4$ and TiO_2-F are presented in Figure 4. In this figure it can be seen completely different morphologies; $MgFe_2O_4$ particles present are cubic shapes with a mean size of 90 nm. While for the TiO_2-F sample ellipsoidal particles with an average size of 20 nm can be observed. These results, as in the case of the crystal size calculations, are to be expected as various methods of synthesis were used, which correspond to different mechanisms of nucleation and particle growth.

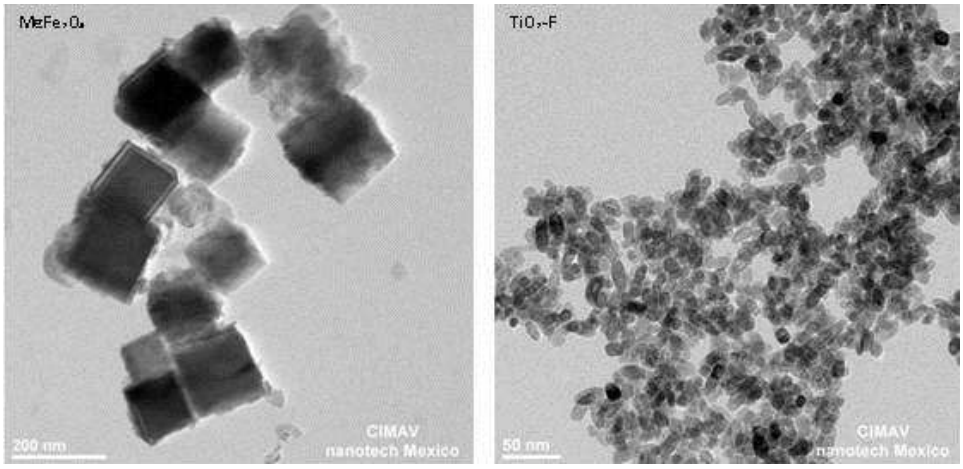

Fig 4. TEM images for the samples $MgFe_2O_4$ and TiO_2-F

3.4. Nitrogen Physisorption (BET)

The method of nitrogen physisorption (BET) was employed for obtaining the surface area of the synthesized materials ($MgFe_2O_4$ and TiO_2-F). Figure 5 shows the adsorption isotherms, where it appears that TiO_2-F isotherm is of type IV according to the classification of the IUPAC, which is characteristic of mesoporous materials, with a H2 hysteresis loop characteristic bottleneck type pores. However, the adsorption isotherm for $MgFe_2O_4$ is of type III characteristic of a hysteresis loop H3 of mesoporous materials with a very wide size distribution [21], which can be associated with interparticle porosity, very characteristic of materials obtained by precipitation.

Moreover, in Figure 5 it can be observed that there is a considerable difference in the amount of adsorbed nitrogen, being higher for the sample TiO_2-F, this is attributed to presenting greater surface area. This result was expected since by size particle (small) as well as by porosity high surface areas are generated. The value of the specific surface area and the particle size obtained by TEM images for each material is presented in Table 1.

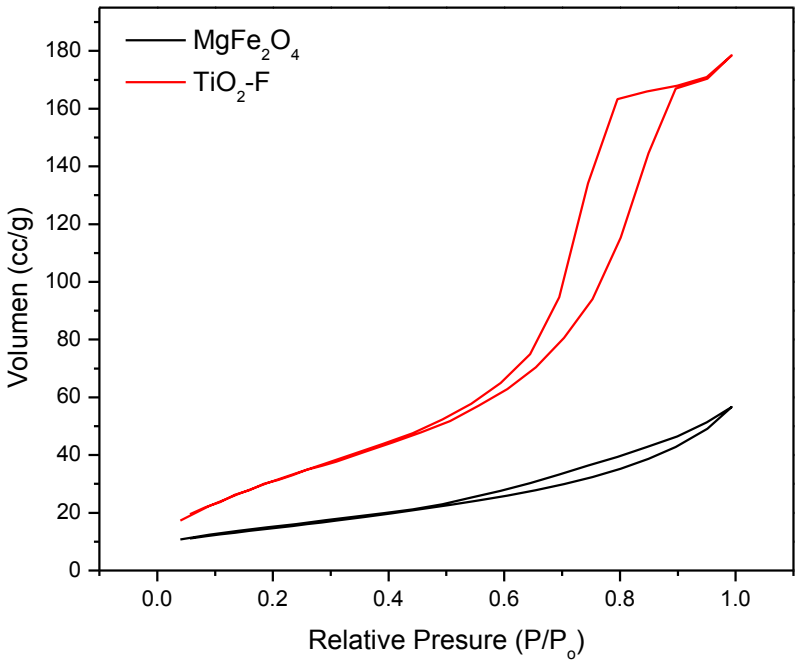

Fig 5. $MgFe_2O_4$ and TiO_2-F adsorption isotherms.

Table 1. BET surface area and particle size for the synthesized photocatalysts

Sample	Area (m_2/g)	Particle size (nm)
TiO_2-F	124	20
$MgFe_2O_4$	53	90

3.5. Photocatalytic Evaluation

In Figure 6 the hydrogen evolution of both $MgFe_2O_4$ and TiO_2-F samples are presented. It is evident that an increased hydrogen production for sample $MgFe_2O_4$ was achieved, although it has less surface area than the TiO_2-F, the photocatalytic activity mainly is attributed to the lower value of Eg, which is in the range of visible light as mentioned in Figure 3. More than 650 $\mu molH_2/g_{cat}$ was reached for sample $MgFe_2O_4$ after 8 h of irradiation against 15 $\mu molH_2/g_{cat}$ produced by the synthesized TiO_2-F.

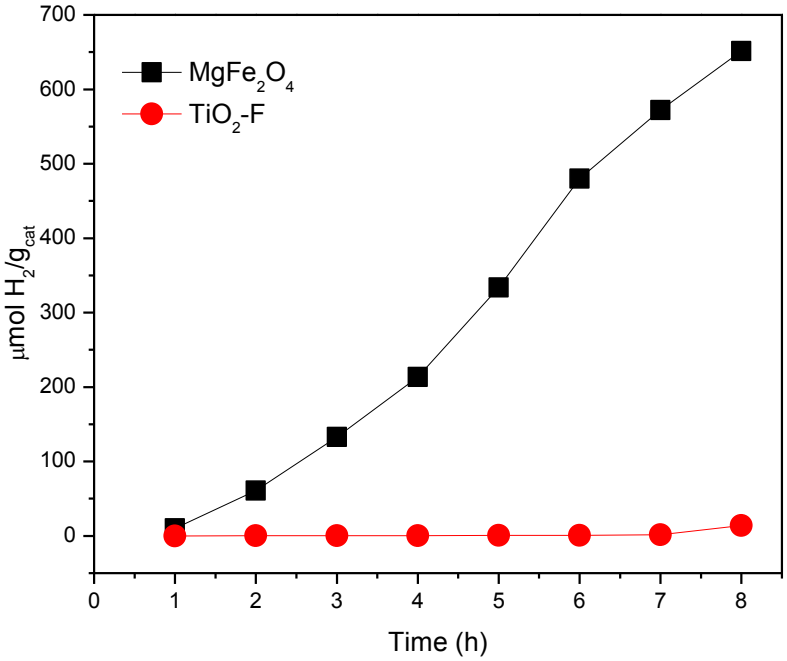

Fig 6. Photocatalytic evaluation for the production of H_2

4. Summary and perspectives

Magnesium ferrite was synthesized by coprecipitation and hydrothermal treatment, resulting in a mixture of phases ($MgFe_2O_4$ and Fe_2O_3), while TiO2-F sample was obtained by sol-gel assisted with hydrothermal treatment, reaching the pure anatase phase. Results obtained by diffuse reflectance UV-Vis spectroscopy showed the Eg value for the ferrite was located in the visible region, 2.07 eV (599nm). TEM results show particle sizes in the nanometer range in both cases, and also indicated a cubic morphology for $MgFe_2O_4$, while ellipsoidal particles for TiO2-F. The photocatalytic evaluation results for the H_2 production indicate a higher activity for the $MgFe_2O_4$ sample, with a maximum production of 650 $\mu molH_2/g_{cat}$ over a period of 8, while TiO_2-F only achieved a production of 15 $\mu molH_2/g_{cat}$. This is due to the fact that magnesium ferrite is able to be activated under the visible light range.

Acknowledgements

Finally, thanks to technicians Maria Teresa Chaparro, Enrique Torres, Luis de la Torre and Carlos Ornelas for their contributions to the of UV-Vis spectroscopy, BET area, X-ray diffraction and scanning electron microscopy results. As well as the Centro de Investigación en Materiales Avanzados S. C. for the support in the use of its infrastructure.

References

[1] Thammanoon Sreethawong, Yoshikazu Suzuki, Susumu Yoshikawa., Photocatalytic evolution of hydrogen over mesoporous TiO_2 supported NiO photocatalyst prepared by single-step sol–gel process with surfactant template. International Journal of Hydrogen Energy 30 (2005) 1053 – 1062

[2] BilgeYildiz∗, Mujid S. Kazimi., Efficiency of hydrogen production systems using alternative nuclear energy technologies. International Journal of Hydrogen Energy 31 (2006) 77 – 92

[3] Jum Suk Janga, Hyun Gyu Kimb, Pramod H. Borsea, Jae Sung Leea, Simultaneous hydrogen production and decomposition of H_2S dissolved in alkaline water over $CdS.TiO_2$ composite photocatalysts under visible light irradiation. International Journal of Hydrogen Energy 32 (2007) 4786 – 4791

[4] A. Kudo, Development photocatalyst materials for water splitting, International Journal of Hydrogen Energy 31 (2006) 197 – 202

[5] K. Domen, M. Hara, J.N. Kondo, T. Takata, A. Kudo, H. Kobayashi *et al.* New aspects of heterogeneous photocatalysts for water decomposition, Korean J Chem Eng, 18 (2001) 862–866.

[6] Kim, D.W. Hwang, J.S. Lee, An undoped, single phase oxide photocatalyst working under visible light J Am Chem Soc 126 (2004) 8912–8913

[7] H.G. Kim, P.H. Borse, W. Choi, J.S. Lee, Photocatalytic nanodiodes for visible light photocatalysis Angew Chem Int Ed, 44 (2005) 4585–4589.

[8] H. Zazoua, A. Boudjemaa, R. Chebout and K. Bachari, Enhanced photocatalytic hydrogen production under visible light over a material based on magnesium ferrite derived from layered double hydroxides (LDHs), Int. J. Energy Res. (2014)

[9] Erik Casbeer, Virender K. Sharma, Xiang-Zhong Li, Synthesis and photocatalytic activity of ferrites under visible light: A review, Separation and Purification Technology 87 (2012) 1–14

[10] Kullarni RG, Joshi HH, Comparison of magnetic properties of $MgFe_2O_4$ prepared by wet-chemical and ceramic methods, J Solid State Chem 64(2) (1986), 141

[11] Lakshman A, Rao KH, Mendiratta RG, Magnetic properties of In3+ and Cr3+ substituted Mg–Mn ferrites, J Magn Magn Mater 250 (2002), 92

[12] 0. Chhaya SD, Pandya MP, Chhantbar MC, Modi KB, Baldha GJ, Joshi HH, Study of substitution limit, structural, bulk magnetic and electrical properties of Ca^{2+} substituted magnesium ferrite, J Alloys Comp 377 (2004) 155.

[13] Verma S, Joy PA, Khollam YB, Potdar HS, Deshpande SB, Synthesis of nanosized $MgFe_2O_4$ powders by microwave hydrothermal method, Mater Lett (2004) 1092

[14] Oliver SA, Willey RJ, Hamdeh HH, Oliveri G, Busca G Scripta, Structure and magnetic properties magnesium ferrite fine powders**,** Metal Mater 33(10/11), (1995) 1695

[15] Basahel SN, El-Bellihi AA, Gabal M, Diefallah El-HM, Thermal decomposition of iron(III) oxalate-magnesium oxalate mixtures, Thermochim Acta 256(2) (1995) 339

[16] Patil KC, Gajapathy D, Pai Verneker VR., Low temperature cobaltite formation using mixed metal oxalate hydrazinate precursor Mater Res Bull 17 (1982) 29

[17] Rupard RG, Gallagher PK,The thermal-decomposition of coprecipitates and physical mixtures of magnesium-iron oxalates, Thermochim Acta 272 (1996) 11

[18] Sepelak V, Baabe D, Mienert D, Litterst FJ, Becker KD, Enhanced magnetisation in nanocrystalline high-energy milled $MgFe_2O_4$, Scripta Mater 48 (2003) 91

[19] Chen Q, Rondinone AJ, Chakoumakos BC, Zhang ZJ, Synthesis of superparamagnetic $MgFe_2O_4$ nanoparticles by coprecipitation. J Magn Magn Mater 194 (1999) 1

[20] O.-Bong Yanga, M. Alam Khana, Seong Ihl Woob Hydrothermally stabilized Fe(III) doped titania active under visible light for water splitting reaction international journal of hydrogen energy 33 (2008) 5345–5351**.**

[21] Bruno Clair, Shan-Shan Chang, Julien Ruelle, Jacques Beauchene, Francesco Di Renzo, Francxoise Quignard, Guang-Jie Zhao, Hiroyuki Yamamoto and Joseph Gril, Mesoporosity as a new parameter for understanding tensión stress generation in trees Journal of Experimental Botany Advance Access 12 (2009).

[22] Shuxi Dai, Yanqiang Wu, Toshio Sakai, Zuliang Du, Hideki Sakai, Masahiko Abe, Preparation of Highly Crystalline TiO_2 Nanostructures by Acid-assisted Hydrothermal Treatment of Hexagonal-structured Nanocrystalline Titania/Cetyltrimethyammonium Bromide Nanoskeleton, Nanoscale Res Lett (2010) 5:1829–1835.